

FIRST-PRINCIPLES CALCULATION OF THE DYNAMICAL AND THERMODYNAMIC PROPERTIES OF CuInSe₂

Y. YU*, G. D. ZHAO, X. L. ZHENG, Z. R. WEI

College of Optoelectronic Technology, Chengdu University of Information Technology, Chengdu 610225, China

We have performed detailed studies of the lattice dynamics and thermodynamic properties of CuInSe₂ within the density functional perturbation theory and pseudopotential methods. The phonon frequencies at the \tilde{A} point of the Brillouin zone are calculated and their symmetry assignments are given. The calculated Raman and infrared active phonon frequencies are in excellent agreement with the experimental values and other calculations. The results for the phonon dispersion curves of CuInSe₂ along several high-symmetry lines together with the corresponding phonon density of states are displayed. The thermodynamic properties including the phonon contribution to the Helmholtz free energy ΔF , the phonon contribution to the internal energy ΔE , the entropy S , and the constant-volume specific heat C_V are determined within the harmonic approximation based on the calculated phonon dispersion relations.

(Received November 8, 2015; Accepted January 9, 2016)

Keywords: CuInSe₂, DFPT, lattice dynamics, thermodynamic

1. Introduction

There is much current interest in thin film solar cells as part of the total research and development effort into solar cells. One of the most promising materials for thin film solar cells is CuInSe₂. It is a direct energy gap semiconductor (about 1.0 eV at room temperature) which has attracted much attention in the past decades because it is known to be a promising semiconductor for the fabrication of high-efficiency thin-film solar cells due to its high absorption coefficient (about $5 \times 10^5 \text{ cm}^{-1}$), suitable band gap and good chemical stability [1-3].

The thermodynamic properties are one of the most basic properties of any material. Thermal properties of solids depend on their lattice dynamical behaviour. In spite of significant effort devoted to gain a better and deeper understanding of the electrical and optical properties of CuInSe₂, the data related to its lattice vibrations are scarce. And what's more, controversy exists on the results of phonon dispersion curves reported by different authors. The lattice dynamical properties of CuInSe₂ have been studied for the last four decades by a number of experimental and theoretical methods. Experimentally, the first Raman (R) and infrared (IR) spectra of CuInSe₂ were reported in 1976 [4], but the results were inconsistent with existing Raman and infrared spectra [5-11]. Later the reports [5-9] on the investigation of the infrared spectra and the Raman scattering appeared, which agreed in a better way among themselves. However, not all vibrational modes in infrared spectra and Raman scattering have been found. The most complete analysis of vibrational

* Corresponding author: yy2012@cuit.edu.cn

properties of CuInSe_2 crystals was given in Refs. [7-11]. On the theoretical side, there have been only a few attempts to calculate the lattice dynamical by first-principles methods [12-14] and a detailed knowledge is still lacking. The phonon dispersion relations and phonon density of states of CuInSe_2 were calculated using the direct method by Lazewski *et al.* [12]. Postnikov *et al.* [13] investigated the lattice dynamics of CuInSe_2 by frozen-phonon method. The understanding of the material has benefited greatly from the availability of first-principles methods for calculating phonon properties. Generally, these methods can be classified into two main types: the direct (or frozen-phonon) [15, 16] approach and the linear-response approach [17, 18]. In the former approach, the properties of phonons at commensurate wave vectors are obtained from supercell calculations of forces or total-energy changes between equilibrium and distorted structures. In the latter approach, based on density-functional perturbation theory (DFPT) [19, 20], expressions are derived for the second derivatives of the total energy with respect to atomic displacements and these are calculated by solving a Sternheimer equation [17] or by using minimization methods [18]. Compared to the direct approach, the linear-response approach has important advantages in that time-consuming supercell calculations are avoided and phonons of arbitrary wave vector can be treated with a cost that is independent of wave vector. The dynamical properties of CuInSe_2 have been studied using linear-response approach by Parlak *et al.* [14]. Although the phonon frequencies are calculated, the thermodynamic properties of CuInSe_2 are not given.

The purpose of this paper is to obtain in more detail the dynamical and thermodynamic properties of CuInSe_2 using the density functional perturbation theory. Our calculations start with the structural optimization and check that our relaxed structural parameters are consistent with the experimental work. The phonon frequencies and phonon density of states (DOS) are then computed from linear response techniques. Finally, the phonon contribution to the Helmholtz free energy ΔF , the phonon contribution to the internal energy ΔE , the entropy S , and the constant-volume specific heat C_V are calculated by varying only the temperature of the thermal occupation number in the corresponding formula. In the following, we describe the calculation methods and discuss the results.

2. Computational details

All of the results reported in this paper were obtained by using ABINIT [21] implementation of the density-functional theory (DFT) and density-functional perturbation theory with a plane-wave basis set for the electronic wave functions and periodic boundary conditions. It relies on an efficient fast Fourier transform algorithm [22] for the conversion of wave functions between real and reciprocal spaces, on an adaptation to a fixed potential of the band-by-band conjugate-gradient algorithm [23], and on a potential-based conjugate-gradient method [24] for the determination of the self-consistent potential. The interaction between the valence electrons and the nuclei and core electrons is described by Troullier-Martins type norm-conserving pseudopotentials which have been generated thanks to the FHI98PP code [25]. The exchange-correlation energy is evaluated in local density approximation (LDA), using Perdew-Wang parametrization [26] of Ceperley-Alder electron-gas data [27]. Cu pseudopotential includes the 3d and 4s in valence, In pseudopotential includes the 5s and 5p in valence, for Se pseudopotential, 4s and 4p are taken as the valence states.

All the calculations involve an eight-atom tetragonal primitive cell. The original lattice constants and internal coordinate used in our calculations are taken from the experimental values. For the optimizations, the wave functions are expanded in plane waves up to a kinetic energy cutoff of 36 hartree. Integrals over the Brillouin zone (BZ) are replaced by a sum on a Monkhorst-pack grid of $4 \times 4 \times 4$ special k -point. After geometry optimizations, the relaxed structures are used in the dynamical calculations to obtain the phonon frequencies and phonon density of states. The thermodynamic functions of CuInSe_2 can be determined by the entire phonon spectrum.

3. Results and discussion

3.1 Structural optimization

CuInSe_2 belongs to the ternary $A^{\text{I}}B^{\text{III}}C^{\text{VI}}_2$ chalcopyrite family of compounds. These materials crystallize in the chalcopyrite type structure (s. g. $\bar{I}42d$), which can be derived from the sphalerite structure by doubling the unit cell in the z direction. Each anion is coordinated by two A and two B cations, whereas each cation is tetrahedrally coordinated by four anions. Generally, I-VI and III-VI bond lengths, denoted by $d_{\text{I-VI}}$ and $d_{\text{III-VI}}$, respectively, are not equal, mentioned substitution results in two different structural deformations: the first one is the relocation of anions in the x - y plane which is characterized by parameter $u = 0.25 + (d_{\text{I-VI}}^2 - d_{\text{III-VI}}^2) / a^2$. Here, a is the lattice constant in the x or y direction. The second consequence of differing anion-cation bond lengths is a deformation of the unit cell along the z axis to a length c which is generally different from $2a$. This tetragonal distortion is characterized by the quantity c/a .

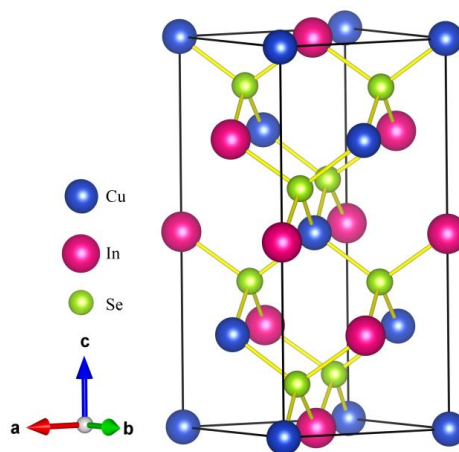


Fig. 1 Crystal structure of CuInSe_2 (chalcopyrite-type; body-centered tetragonal- $\bar{I}42d$)

The body-centered tetragonal structure of CuInSe_2 is shown in Fig. 1. The unit and primitive cells contain four and two formula units, respectively. Ion positions can be generated using the following minimum set of (x, y, z) coordinates expressed in units of the a and c constants.

Group I: (0, 0, 0), (0, 1/2, 1/4)

Group III: (0, 0, 1/2), (0, 1/2, 3/4)

Group VI: (u , 1/4, 1/8), ($-u$, 3/4, 1/8), (3/4, u , 7/8), (1/4, $-u$, 7/8)

The zero pressure lattice structural properties are obtained by energy and force minimization and compared to the available calculated and experimental values in Table 1. Considering that the zero-point motion and thermal effects are not taken into account, the calculated lattice parameters agree quite well with the experimental ones. Our calculations underestimate the equilibrium lattice parameter a (c) with the maximal error of 0.89-1.45% (0.74-0.89%) with respect to experimental values, a normal agreement by LDA standards. This is largely sufficient to allow the further study of vibrational and thermodynamic properties.

Table 1 The equilibrium lattice constant a (c) (in Å), axial ratio c/a , cell volume V (Å³) and internal parameter for CuInSe₂.

Method	a	c	c/a	u
Present work (ABINIT-LDA)	5.731	11.531	2.012	0.216
CASTEP-LDA (Ref. [12])	5.832	11.622	1.993	0.222
WIEN2K-GGA (Ref. [13])	5.733	11.524	2.010	0.220
SIESTA-LDA (Ref. [13])	5.758	11.575	2.010	0.220
VASP-Hybrid (Ref. [28])	5.839	11.754	2.013	0.2259
VASP-GGA (Ref. [28])	5.880	11.831	2.012	0.2177
LAPW-LDA (Ref. [29])	5.768	11.628	2.016	—
ABINIT-LDA (Ref. [14])	5.562	11.135	2.002	0.237
Exp. (Ref. [30])	5.784	11.616	2.008	0.224
Exp. (Ref. [31])	5.782	11.620	2.010	0.235
Exp. (Ref. [32])	5.814	11.634	2.001	0.2258

3.2 Vibrational properties

A crystal lattice with n atoms per unit cell has $3n$ branches, three of which are acoustic and the remainder optical. The chalcopyrite unit cell contains eight atoms giving rise to twenty-four modes of vibrations. Of these twenty-four modes, twenty-one are optic phonon modes and three are acoustic modes. A detailed discussion of group theoretical properties of chalcopyrite zone center phonons can be found in Ref. 9. The irreducible representation at the center of the Brillouin zone is

$$\Gamma_{aco} = 1B_2 + 1E$$

for acoustic modes, and

$$\Gamma_{opt} = 1A_1 + 2A_2 + 3B_1 + 3B_2 + 6E$$

for optical modes. All the optical modes, except A_2 , are Raman active while only B_2 and E modes are IR active. Both B_2 and E modes belong to vector transforming representation, and inclusion of the long-rang polarization interaction results in splitting of these modes into transverse-optical (TO)

and longitudinal-optical (LO) components giving nine polar vibrations. Three B_2 modes with polarization are along the c -axis (the optic axis), and six E modes are perpendicular to this axis. This results in different numbers of IR modes being active for $E//c$ and $E\perp c$. Optical modes having A_1 and A_2 symmetry involve only displacement of anions. B_1 , B_2 and E symmetry modes include displacement of cation, as well. The IR active B_2 mode involves in-phase motion of each cation pair and that of two anion pairs along principal axis and as a result has a dipole moment in that direction. For the IR active E mode, the resultant motion of each cation pair and that of each anion pair are along either the x or the y axis which causes twofold degeneracy and a dipole moment in the x - y plane. The A_1 and B_1 modes are out of phase motion of ions and they do not have a dipole moment, so they are not IR active but Raman active. The A_2 mode is out of phase motion of anion pairs and does not produce a dipole moment.

The calculated zone-center (Γ point) phonon frequencies of CuInSe_2 and their symmetry assignments are displayed and compared with Raman [9], infrared [10] and neutron [11] spectroscopic measurements and other calculations [11, 12, 14] in Table 2. Our result includes LO/TO splitting, which is determined by the effective charge tensors and electronic dielectric constant. As can be seen from Table 2, the zone-center phonon frequencies for CuInSe_2 are clearly grouped into three groups: low (57 - 78 cm^{-1}), medium (150 - 163 cm^{-1}), and high frequency (176 - 220 cm^{-1}). The results for the phonon dispersion curves of CuInSe_2 along several high-symmetry lines together with the corresponding phonon density of states (DOS) are displayed in Fig. 2. Our calculations show that the spectra of the crystal consist of three bands and have the limit at about 220 cm^{-1} . One finds that a clear gap opens between the 6 upper energy branches and the remaining 18 dispersion branches. The frequency rang of atomic vibrations in CuInSe_2 is in accord with the typical 50 - 500 cm^{-1} for the $A^I B^III X_2^{VI}$ and $A^{II} B^{IV} X_2^V$ compounds [33].

Table 2 Phonon frequencies (unit: cm^{-1}) at zone-center (Γ point) of CuInSe_2 .

Mode		Frequency LO/TO cm^{-1}							
		Theory Present	Experiment				Theory		
			Ref. 11	Ref. 10	Ref. 9 300 K	Ref. 9 100 K	Ref. 11	Ref. 12	Ref. 14
E	R, IR	216/210	215	227/204	230/217	233/217	227/219	244/215	237/223
	R, IR	208/206	198	174/162	— / —	230/227	210/202	214/210	224/219
	R, IR	204/196	181	128/122	— /211	216/211	187/180	204/197	207/204
	R, IR	150/150	136	116/108	— / —	188/188	135/135	150/150	155/155
	R, IR	72/72	70	77/71	77/77	78/78	71/70	71/70	76/75
	R, IR	57/57	53	57/55	60/58	60/61	53/53	52/52	59/59
B ₂	R, IR	220/216	238	228/208	233/215	233/217	244/217	238/216	242/228
	R, IR	196/193	194	169/163	198/—	200/177	192/176	215/198	204/198
	R, IR	68/67	55	79/70	71/70	72/70	56/53	73/66	71/70
B ₁	R	218	207	—	—	229	209	220	228
	R	163	159	—	—	179	156	163	184
	R	78	62	—	—	67	63	77	70
A ₂	Silent	191	197	—	—	—	198	186	200
	Silent	177	161	—	—	—	161	176	168
A ₁	R	176	178	—	176	178	177	177	185

The Raman data by Gan *et al.* [4] are completely different from ours. Tanino *et al.* have measured Raman spectra of CuInSe_2 single crystals at room and low temperatures [9]. They observed more vibration modes and LO/TO splitting at 100 K. Our calculated value for A₁ mode which involves the motion of only the anions is 176 cm^{-1} which is in good agreement with the experimental values. We note that, from previous infrared studies performed at room temperature in the experimental rang $50\text{-}500 \text{ cm}^{-1}$, A₂ was not observed. A₂ modes predicted by group theory were calculated, and our calculated value for A₂ is in good agreement with other calculations, especially Refs. [12]. In the experiment, the A₂ modes were only measured by inelastic neutron scattering [11]. Each one of three B₁ mode frequencies is in low, medium, and high frequency region.

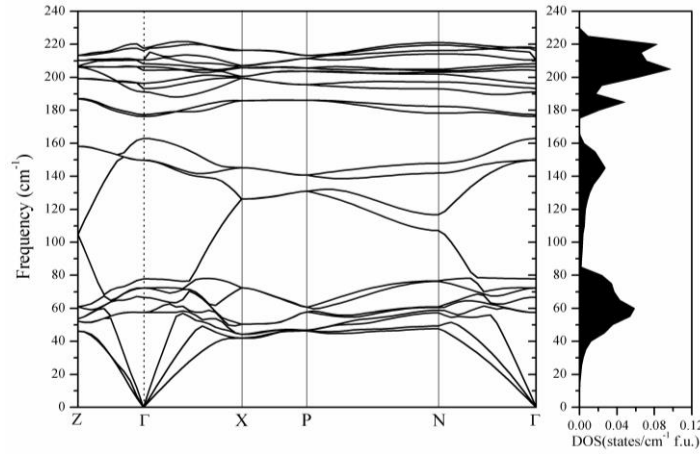


Fig. 2 Calculated phonon dispersion curves along symmetry lines in the Brillouin zone and the corresponding phonon density of states (DOS) for CuInSe_2 .

As can be observed from Fig. 2, the calculated LO-TO mode splitting of B_2 and E modes are small, ranging from 0 to 8 cm^{-1} . The splitting for the low frequency modes is small and even zero, because the low frequency modes are essentially the folded acoustic modes, they correspond to whole molecular units moving relative to each other. On the other hand, the high frequency modes involve individual atoms moving against each other which produce higher dipole moments which lead to higher splitting. This is the similar splitting case with CuGaSe_2 reported in Ref. 34.

3.3 Thermodynamic properties

The knowledge of the entire phonon spectrum granted by DFPT makes possible the calculation of several important thermodynamic properties as functions of temperature T . In the present work, the phonon contribution to the Helmholtz free energy ΔF , the phonon contribution to the internal energy ΔE , the entropy S , and the constant-volume specific heat C_V , at temperature T are calculated using the formulas in Ref. 35 within the harmonic approximation. The calculated phonon contribution to the Helmholtz free energy ΔF and the phonon contribution to the internal energy ΔE of CuInSe_2 are shown in Fig. 3. The ΔF and ΔE are usually calculated within harmonic approximation:

$$\Delta F = 3n N \frac{\hbar}{k_B} \int_0^{\omega_{\max}} \ln \left\{ 2 \sinh \frac{\hbar \omega}{2k_B T} \right\} g(\omega) d\omega, \quad (1)$$

and

$$\Delta E = 3nN \frac{\hbar}{2} \int_0^{\omega_{\max}} \omega \coth \left(\frac{\hbar \omega}{2k_B T} \right) g(\omega) d\omega. \quad (2)$$

ΔF and ΔE at zero-temperature represent the zero-point motion, which can be calculated from the expression as

$$\Delta F_0 = \Delta E_0 = 3nN \int_0^{\omega_{\max}} \frac{\hbar \omega}{2} g(\omega) d\omega, \quad (3)$$

where n is the number of atoms per unit cell, N is the number of unit cells, ω is the phonon frequencies, ω_{\max} is the largest phonon frequency, and $g(\omega)$ is the normalized phonon density of states with $\int_0^{\omega_{\max}} g(\omega)d\omega = 1$. The calculated $\Delta F_0 = \Delta E_0 = 10.2$ KJ/mol for CuInSe₂.

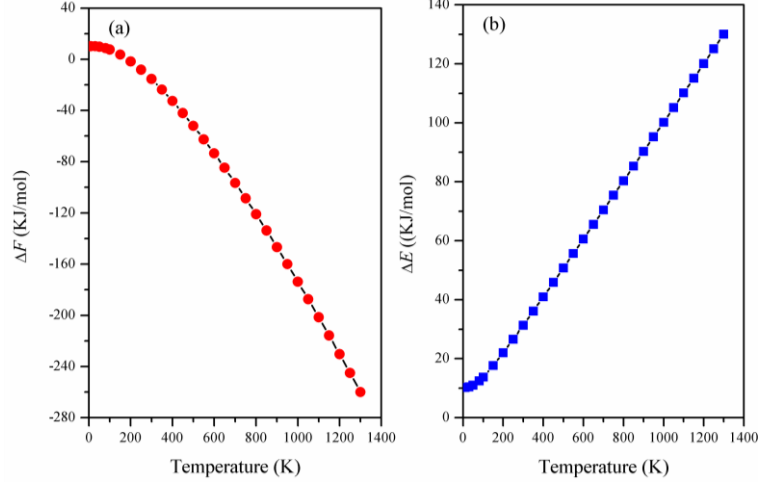


Fig. 3 The calculated phonon contribution to the Helmholtz free energy ΔF (a) and the phonon contribution to the internal energy ΔE (b) of CuInSe₂.

Quantitatively, the entropy is defined by the formulas

$$S = 3n N k_B \int_0^{\omega_{\max}} \left[\frac{\hbar\omega}{2k_B T} \coth \frac{\hbar\omega}{2k_B T} - \ln \left\{ 2 \sinh \frac{\hbar\omega}{2k_B T} \right\} \right] \times g(\omega) d\omega. \quad (4)$$

From Fig. 4, it can be seen that the calculated entropies of CuInSe₂ exhibit reasonable agreement with the experimental values [36, 37] below room temperature. The experimental values are slightly larger by about 2% than the calculated values since the effects of anharmonicity are ignored and the theoretical lattice constants are used in the calculation.

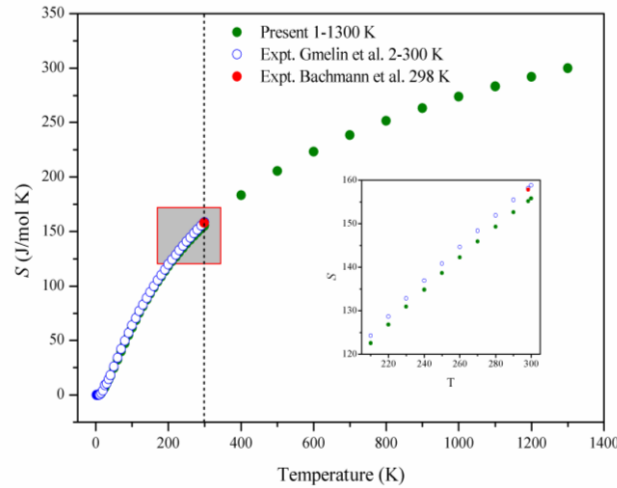


Fig. 4 The comparison between the calculated and experimental entropy of CuInSe_2 .

Within harmonic approximation, C_V is given as

$$C_V = 3nNk_B \int_0^{\omega_{\max}} \left(\frac{\hbar\omega}{2k_B T} \right)^2 \text{csc}^2 \left(\frac{\hbar\omega}{2k_B T} \right) g(\omega) d\omega. \quad (5)$$

The constant-volume specific heats C_V are calculated and shown in Fig. 5. In the low-temperature limit, the specific heat exhibits the T^3 power-law behaviour, and approaches at high temperature the classical asymptotic limit of $C_V=3nk_B=100 \text{ J/mol K}$. Bachmann *et al.* [37] calculated the C_V which derived from the experimental data at constant pressure according to formula. As shown in Fig. 5, the calculated C_V of CuInSe_2 exhibits reasonable agreement with the values [36, 37] calculated by Bachmann *et al.* in the temperature range $1 \text{ K} \leq T \leq 40 \text{ K}$. The discrepancies between the calculated harmonic specific heat C_V and the experimental specific heat C_p above $\sim 200 \text{ K}$ are indicative of vibrational anharmonicity, shown in Fig. 5. The relation C_p and C_V is determined by $C_p - C_V = \alpha_v^2(T)B_0VT$, where α_v is the volume thermal expansion coefficient, B_0 is the bulk modulus, V is the volume and T is absolute temperature. In order to deduce the theoretical C_p , the determination of thermal expansion coefficients is necessary, which is in progress.

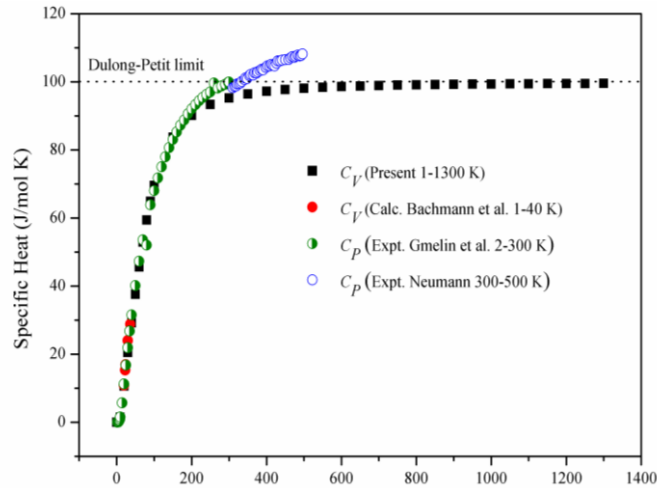


Fig. 5 The comparison between the calculated and experimental specific heat of CuInSe_2 .

4. Conclusions

In summary, we have investigated the lattice dynamics and thermodynamic properties of ternary semiconductor CuInSe_2 within the density functional perturbation theory framework. Firstly, the structural parameters, including the internal coordinates, are relaxed, and excellent agreement is achieved with experimental results. The vibrational modes at the center of the Brillouin zone have been evaluated and compared with experiment. All the Raman-active and infrared-active modes (including LO-TO splitting) are identified and compared with experiments and previous theoretical calculations. The calculated zone-center phonon mode frequencies are in good agreement with infrared, Raman and neutron scattering experiments. Finally, the thermodynamic properties including the phonon contribution to the Helmholtz free energy ΔF , the phonon contribution to the internal energy ΔE , the entropy S , and the constant-volume specific heat C_V are determined within the harmonic approximation based on the calculated phonon density of states. The calculated entropy S and specific heat C_V of CuInSe_2 exhibit reasonable agreement with the experimental values.

Acknowledgments

This work was supported by the Open Research Fund of Computational Physics Key Laboratory of Sichuan Province (No. JSWL2014KFZ01), Yibin University, and Scientific Research Foundation of Chengdu University of Information Technology (No. CRF201502).

References

- [1] J. P. Benner, L. Kazmerski, IEEE Spectrum **36**, 34 (1999).
- [2] A. Rockett, R.W. Birkmire, J. Appl. Phys. **70**, R81 (1991).
- [3] S. Schorr, G. Geandier, Cryst. Res. Technol. **41**, 450 (2006).

- [4] J.N. Gan, J. Tauc, V.G. Lambrecht, M. Robbins, *Phys. Rev. B* **13**, 3610 (1976).
- [5] H. Neumann, R.D. Tomlinson, W. Kissinger, N. Avgerinos, *Phys. Status Solidi B* **118**, K51 (1983).
- [6] H. Neumann, H. Sobotta, V. Riede, B. Schumann, G. Kuhn, *Crystal Res. Technol.* **18**, K90 (1983).
- [7] H. Neumann, *Sol. Cells* **16**, 399 (1986).
- [8] C. Rincon, F.J. Ramirez, *J. Appl. Phys.* **72**, 4321 (1992).
- [9] H. Tanino, T. Maeda, H. Fujikake, H. Nakanishi, S. Endo, T. Irie, *Phys. Rev. B* **45**, 13323 (1992).
- [10] N.N. Syrbu, M. Bogdanash, V.E. Tezlevan, I. Mushcutariu, *Physica B* **229**, 199 (1997).
- [11] P. Derollez, R. Fouret, A. Laamyem, B. Hennion, J. Gonzalez, *J. Phys.: Condens. Matter* **11**, 3987 (1999).
- [12] J. Lazewski, K. Parlinski, B. Hennion, R. Fouret, *J. Phys.: Condens. Matter* **11**, 9665 (1999).
- [13] A.V. Postnikov, M.V. Yakushev, *Thin Solid Films* **451-452**, 141 (2004).
- [14] C. Parlak, R. Eryigit, *Phys. Rev. B* **66**, 165201 (2002).
- [15] K. Parlinski, Z.-Q. Li, Y. Kawazoe, *Phys. Rev. Lett.* **78**, 4063 (1997).
- [16] K. Kunc, R.M. Martin, *Phys. Rev. Lett.* **48**, 406 (1982).
- [17] P. Giannozzi, S. de Gironcoli, P. Pavone, S. Baroni, *Phys. Rev. B* **43**, 7231 (1991).
- [18] X. Gonze, C. Lee, *Phys. Rev. B* **55**, 10355 (1997).
- [19] S. Baroni, P. Giannozzi, A. Testa, *Phys. Rev. Lett.* **58**, 1861 (1987).
- [20] S. Baroni S. de Gironcoli, A. Dal Corso, P. Giannozzi, *Rev. Mod. Phys.* **73**, 515 (2001).
- [21] X. Gonze, J.-M. Beuken, R. Caracas, F. Detraux, M. Fuchs, G.-M. Rignanese, L. Sindic, M. Verstraete, G. Zerah, F. Jollet, M. Torrent, A. Roy, M. Mikami, Ph. Ghosez, J.-Y. Raty, D.C. Allan, *Comput. Mater. Sci.* **25**, 478 (2002). <http://www.abinit.org>.
- [22] S. Goedecker, *SIAM J. Sci. Comput. (USA)* **18**, 1605 (1997).
- [23] M.C. Payne, M.P. Teter, D.C. Allan, T.A. Arias, J.D. Joannopoulos, *Rev. Mod. Phys.* **64**, 1045 (1992).
- [24] X. Gonze, *Phys. Rev. B* **54**, 4383 (1996).
- [25] M. Fuchs, M. Scheffler, *Comput. Phys. Commun.* **119**, 67 (1999).
- [26] J.P. Perdew, Y. Wang, *Phys. Rev. B* **45**, 13244 (1992).
- [27] D.M. Ceperley, B.J. Alder, *Phys. Rev. Lett.* **45**, 566 (1980).
- [28] J. Pohl and K. Albe, *J. Appl. Phys.* **108**, 023509 (2010).
- [29] S.B. Zhang, S.-H. Wei, A. Zunger, H. Katayama-Yoshida, *Phys. Rev. B* **57**, 9642 (1998).
- [30] H.W. Spiess, U. Haeblerl, G. Brandt, A. Rauber, J. Schneider, *phys. Stat. sol. (b)* **62**, 183 (1974).
- [31] J. Parkes, R.D. Tomlinson, M.J. Hampshire, *J. Appl. Cryst.* **6**, 414 (1973).
- [32] K. Takarabe, K. Kawai, K. Kawamura, S. Minomura, N. Yamamoto, *J. Cryst. Growth* **99**, 766 (1990).
- [33] F.W. Ohrendorf, H. Haeuseler, *Cryst. Res. Technol* **34**, 339 (1999).
- [34] C. Parlak, R. Eryigit, *Phys. Rev. B* **73**, 245217 (10pp) (2006).
- [35] C. Lee, X. Gonze, *Phys. Rev. B* **51**, 8610 (1995).
- [36] E. Gmelin, W. Honle, *Thermochim. Acta* **269/270**, 575 (1995).
- [37] K.J. Bachmann, F.S.L. Hsu, F.A. Thiel, H.M. Kasper, *J. Electron. Mater.* **6**, 431 (1977).